Research Square

Preprints are preliminary reports that have not undergone peer review.
They should not be considered conclusive, used to inform clinical practice,
or referenced by the media as validated information.

Dimethyl fumarate attenuates cadmium-induced neurobehavioural deficits, NF-κB/NLRP3-associated neuroinflammation and synaptic protein alterations in rats

Samuel Bolaji Mesole

ms361450@gmail.com

Eden University

Alfred Omachonu Okpanachi

Eden University

Oria Sunday Rademene

University of Cross River State

Yusuf Ademola Uthman

Mulungushi University

Mwitwa Kombe

Eden University

Sharon Kaundu

Eden University

Chinyama Jonathan

Eden University

Kafunda Tuesday

Eden University

Kebe Edet Obeten

Lusaka Apex Medical University

Research Article

Keywords: Cadmium, Dimethyl fumarate, Neuroinflammation, NF-κB, NLRP3 inflammasome, Synaptic proteins

Posted Date: August 25th, 2026

DOI: https://doi.org/10.21203/rs.3.rs-10780468/v1

License: This work is licensed under a Creative Commons Attribution 4.0 International License.
Read Full License

Additional Declarations: No competing interests reported.

Abstract

Cadmium (Cd) exposure is associated with cognitive dysfunction, neuroinflammation and synaptic impairment. This study evaluated whether dimethyl fumarate (DMF) attenuates $CdCl_2$-induced neurotoxicity in rats and whether protection is associated with reduced NF-κB/NLRP3-associated inflammatory signalling and preservation of synaptic proteins. Male Wistar rats received Control, $CdCl_2$ (5 mg/kg/day), DMF (25 mg/kg/day) or $CdCl_2$+DMF treatment orally for 30 days (n = 8/group). $CdCl_2$ impaired spatial learning, recognition memory, spontaneous alternation and exploratory activity, increased TNF-α, IL-1β and IL-6, enhanced NF-κB p65 expression/phosphorylation and NLRP3, ASC and cleaved caspase-1, and reduced BDNF, synaptophysin, PSD-95 and NMDAR subunits in the hippocampus and prefrontal cortex. DMF significantly attenuated these behavioural and molecular alterations. These findings indicate that DMF reduces $CdCl_2$-induced neurobehavioural and molecular toxicity in association with suppression of NF-κB/NLRP3-associated inflammatory signalling and preservation of neurotrophic and synaptic protein profiles.

Highlights

• $CdCl_2$ impaired learning, recognition, working memory and exploratory behaviour.

• DMF attenuated $CdCl_2$-associated NF-κB/NLRP3 inflammasome-associated signalling.

• DMF reduced $CdCl_2$-induced elevations in TNF-α, IL-1β and IL-6.

• DMF preserved BDNF and key synaptic proteins in hippocampus and prefrontal cortex.

• DMF protection was substantial but incomplete across selected endpoints.

1. Introduction

Cadmium (Cd), a common environmental contaminant, has been attracting more and more attention because of its neurotoxic effects. Epidemiological studies have linked Cd exposure with a decline in cognitive performance, and experimental studies have demonstrated that Cd exposure can impair learning and memory and damage neuronal integrity in brain regions involved in cognition (Gustin et al., 2018; Wang et al., 2019). Cd exposure lowers adult hippocampal neurogenesis, promotes cell death and leads to impairment of hippocampus-dependent learning and memory in experimental models (Wang et al., 2019). Exposure to $CdCl_2$ was also associated with oxidative stress, increased TNF-α and IL-6, NF-κB activation and structural damage in the hippocampus (El-Kott et al., 2020). Collectively, these findings suggest that the cognitive effects of Cd exposure are unlikely to be the product of a single cellular disturbance, but rather the outcome of interacting inflammatory, glial and synaptic alterations.

This mechanism is particularly important for neuroinflammation. NF-κB is a key regulator of inflammatory gene expression linking cellular stress to the production of pro-inflammatory mediators.

This system can be chronically engaged in the brain, causing persistent cytokine signalling and subsequent inflammatory reactions. Experimental Cd exposure has been shown to trigger NF-κB activation with higher levels of inflammatory cytokines, supporting its role in Cd-induced brain injury (El-Kott et al., 2020). The NLRP3 inflammasome has also garnered increasing attention. The NLRP3 inflammasome is a multi-protein signalling complex consisting of the NLRP3 protein, the adaptor ASC and caspase-1. Once activated this complex leads to caspase-1 processing and maturation of inflammasome-dependent cytokines. In a Cd-exposure paradigm, Cai et al. (2021) observed an increase of NLRP3, ASC and caspase-1 and reported an IL-1β/IκB-α/NF-κB/NLRP3 inflammatory feedback loop indicating NF-κB and NLRP3 signalling may serve as linked components of Cd-induced neuroinflammation.

Microglia and astrocytes respond promptly to variations in the neuronal environment. Continued stimulation of these cells can augment inflammatory signalling and change neural support. In $CdCl_2$-exposed rats, Gök and Deveci (2022) reported increased ionized calcium-binding adaptor molecule 1 (Iba1) and glial fibrillary acidic protein (GFAP) immunoreactivity, consistent with enhanced microglial and astrocytic reactivity in the cerebral cortex. Experimental exposure to Cd has also been linked to gliosis, changes in NMDA receptor signalling, and reductions in synaptic proteins such as synaptophysin and postsynaptic density protein-95 (PSD-95) (Yang et al., 2023). These changes are important as synaptophysin and PSD-95 are key presynaptic and postsynaptic elements of synaptic structure and NMDA receptors play a key role in glutamatergic transmission and synaptic development. Reduced neurotrophic support has been associated with reduced hippocampal brain-derived neurotrophic factor (BDNF) (Batool et al., 2022) which was associated with Cd-induced cognitive impairment. Thus, glial reactivity, inflammatory signalling and changes in neurotrophic and synaptic proteins are physiologically related processes by which Cd may affect cognitive performance.

Of particular relevance in these processes is dimethyl fumarate (DMF), as beyond non-specific antioxidant protection, control of inflammatory signalling is also implicated. DMF decreased the expression of IL-1β, TNF-α and IL-6, and suppressed the inflammatory activation of primary microglial and astrocytic cells (Wilms et al., 2010). In other experimental contexts, DMF has also been shown to reduce NF-κB-driven cytokine production and nuclear translocation of NF-κB subunits in a Nrf2-independent manner (Gillard et al., 2015). This is especially pertinent given that Tastan et al. (2021) demonstrated the reduction of NLRP3 and caspase-1 by DMF, suppression of microglial inflammasome activation and improvement of inflammation-associated behavioural impairments in mice. Additional mechanistic investigations recently indicated that DMF can covalently modify NLRP3 at Cys673 and inhibit inflammasome activation, further suggesting direct interaction between DMF and NLRP3 regulation (Hu et al., 2024). These observations are consistent with a role of DMF in decreasing the inflammatory and synaptic consequences of Cd neurotoxicity.

However, it remains unknown whether DMF can protect against Cd-induced behavioural impairment while reducing NF-κB/NLRP3 inflammasome-associated signalling and alterations in proteins involved in synaptic function. Therefore, the present study investigated the effect of DMF on $CdCl_2$-induced

neurotoxicity in the hippocampus and prefrontal cortex. Behavioural performance, TNF-α, IL-1β and IL-6, NF-κB p65 expression and phosphorylation, NLRP3, ASC and cleaved caspase-1, BDNF and synaptic proteins including synaptophysin, PSD-95, NMDAR1, NMDAR2A and NMDAR2B were assessed. We hypothesized that DMF would attenuate $CdCl_2$-induced behavioural impairment in association with reduced inflammatory signalling and preservation of neurotrophic and synaptic protein profiles.

2. Materials and Methods

2.1 Experimental design and treatment

Thirty-two adult male Wistar rats weighing 180–220 g were obtained from the Animal House, Eden University School of Medicine, Lusaka, Zambia. The animals were housed in solid-bottom polypropylene cages at a density of four rats per cage, with two cages assigned to each experimental group. They were maintained under standard laboratory conditions at 22 ± 2°C, 50–60% relative humidity, and a 12-h light/12-h dark cycle, with free access to standard rodent chow and water. Animals were allowed to acclimatise for 14 days before treatment, during which body weight and general health status were monitored.

All experimental procedures were approved by the Eden University Animal Use Committee (approval no. EDUAUC/2025/07) and conducted in accordance with institutional guidelines for the care and use of laboratory animals. The study was reported in accordance with the ARRIVE 2.0 guidelines.

Thirty-two rats were allocated equally to four experimental groups (n = 8/group): Control, $CdCl_2$, DMF, and $CdCl_2$+DMF. No formal a priori sample-size calculation was performed. The group size was selected with reference to comparable experimental studies employing similar rodent neurotoxicity paradigms and in consideration of the Reduction principle of the 3Rs, while retaining eight independent biological replicates per group for between-group comparisons.

Animals were eligible for randomisation if, following the 14-day acclimatisation period, they were clinically healthy, exhibited normal feeding, drinking, grooming and locomotor behaviour, and had a body weight within the predefined range of 180–220 g. A priori exclusion criteria were the presence of clinically apparent illness or injury before treatment allocation, body weight outside the predefined range at randomisation, or a pre-existing condition judged by the attending animal-care personnel to compromise completion of the experimental protocol. Following randomisation, an animal or individual measurement could be excluded only for a documented major protocol deviation, such as incorrect treatment administration, loss or irretrievable misidentification of a biological sample, or technical assay failure that prevented generation of a valid measurement. Animals were not excluded solely because of an extreme biological value or because treatment-related effects were observed. Any attrition or exclusions occurring after treatment allocation were documented together with the reason and reported for each experimental group.

To minimise potential imbalance in baseline body weight, rats were weighed at the end of the acclimatisation period and ranked according to body weight. The 32 animals were then arranged into eight weight-matched blocks of four rats with similar baseline weights. Within each block, one animal was randomly allocated to each of the four experimental groups, resulting in eight animals per group and comparable baseline body-weight distributions. Following treatment allocation, animals assigned to each group were housed in two cages containing four rats per cage.

The individual rat was considered the experimental unit because treatments were administered to individual animals and behavioural and biochemical measurements were obtained separately from each animal. Cage represented the housing unit and was not treated as an independent experimental replicate.

Treatment allocation was concealed using coded group assignments. The investigator administering the daily treatments, investigators performing behavioural assessments and biochemical assays, and the investigator conducting the statistical analyses were blinded to treatment-group identity. Treatment preparations were identified only by coded labels, and group identities were not revealed until completion of data collection and the prespecified statistical analyses.

The $CdCl_2$ group received cadmium chloride at 5 mg/kg/day, the DMF group received dimethyl fumarate at 25 mg/kg/day, and the $CdCl_2$+DMF group received DMF at 25 mg/kg/day followed 1 h later by $CdCl_2$ at 5 mg/kg/day. $CdCl_2$ was dissolved in distilled water, whereas DMF was freshly suspended in 0.5% carboxymethylcellulose (CMC). Control animals received equivalent volumes of the corresponding vehicles, consisting of 0.5% CMC followed 1 h later by distilled water. All treatments and corresponding vehicles were administered once daily by oral gavage for 30 consecutive days during the light phase and at approximately the same time each day.

The $CdCl_2$ dose was selected based on previous evidence demonstrating neurochemical and neurobehavioural disturbances following repeated oral administration of 5 mg/kg $CdCl_2$ in rats (Oboh et al., 2020). The DMF dose was selected based on previous in vivo studies in which orally administered DMF at 25 mg/kg produced pharmacological and neuroprotective effects associated with cytoprotective signalling (Han et al., 2016; Carlström et al., 2020).

2.2 Behavioural assessment

Behavioural testing was conducted during the final week of treatment in a quiet, temperature-controlled room under constant lighting between 09:00 and 15:00. Rats were allowed to acclimatize to the testing room for at least 30 min before each session. Behavioural apparatuses and objects were cleaned with 70% ethanol and allowed to dry between animals to minimize residual olfactory cues. Behavioural scoring was performed by an investigator blinded to treatment allocation. To maintain consistency across experimental groups, tests were conducted in the following fixed sequence: open-field test, Y-maze, novel object recognition, and Morris water maze.

2.2.1 Open-field test: Each rat was placed individually in the centre of the open-field arena and allowed to explore freely for 5 min. Each animal underwent a single test session. Line crossings and rearing frequency were recorded as measures of locomotor and exploratory activity, respectively.

2.2.2 Y-maze: Spontaneous alternation was assessed by placing each rat at the end of one arm of a three-arm Y-maze and allowing unrestricted exploration for 8 min. An arm entry was recorded only when all four paws entered the arm. Total arm entries were recorded, and spontaneous alternation was calculated as:

Spontaneous alternation (%) = [number of consecutive triads containing entries into all three arms/(total arm entries − 2)] × 100.

Total arm entries were retained as an additional measure of general exploratory activity.

2.2.3 Novel object recognition: Recognition memory was assessed in an opaque square arena measuring 60 × 60 × 40 cm. The procedure comprised habituation, familiarization and retention phases. During habituation, each rat explored the empty arena for 5 min/day on two consecutive days. During familiarization, two identical objects were positioned symmetrically within the arena, approximately equidistant from the walls, and each rat was allowed to explore them for 5 min. After a 24-h retention interval, one familiar object was replaced with a novel object of similar size but differing in shape and surface texture, and the rat was allowed to explore for a further 5 min. The position of the novel object was counterbalanced across animals to minimize positional bias.

Object exploration was defined as directing the nose toward the object at close range, actively sniffing the object, or touching it with the nose or forepaws. Climbing on, leaning against, or sitting on an object was not scored as object exploration. Recognition and discrimination indices were calculated as:

Recognition index (%) = [novel-object exploration time/total object exploration time] × 100

Discrimination index = (novel-object exploration time − familiar-object exploration time)/total object exploration time.

2.2.4 Morris water maze: Spatial acquisition was assessed in a circular pool measuring 150 cm in diameter, containing opaque water maintained at 24 ± 1°C. A circular escape platform measuring 10 cm in diameter was submerged 1–2 cm below the water surface and maintained in a fixed target quadrant, with constant distal visual cues surrounding the pool. Rats received four acquisition trials per day for four consecutive days from varied starting positions. Each trial lasted a maximum of 60 s. Rats that failed to locate the platform within this period were gently guided to it and allowed to remain on the platform for 10–15 s. Escape latency was recorded for each trial and averaged for each animal on each acquisition day.

2.3 Tissue collection and preparation

Euthanasia and brain-tissue collection

The final treatment was administered on Day 30. The final behavioural assessment was conducted approximately 24 h after the final treatment, after which the animals were returned to their home cages and left undisturbed for a further 24 h to minimise acute behavioural-test-associated effects on biochemical endpoints. Thus, tissue collection was performed approximately 48 h after the final treatment and 24 h after completion of the final behavioural assessment. All animals were euthanised during the same predefined time window to minimise potential circadian variation.

Rats were deeply anaesthetised with ketamine (80 mg/kg, i.p.) and xylazine (10 mg/kg, i.p.). Adequate anaesthetic depth was confirmed by absence of the pedal withdrawal reflex. While maintained under deep anaesthesia, animals were euthanised by decapitation using a rodent guillotine, after which the brain was immediately removed and placed on an ice-chilled dissection surface. Deep anaesthesia before the terminal procedure and the method of euthanasia were consistent with accepted principles for humane rodent euthanasia.

The cerebral hemispheres were gently separated along the midline, and the overlying cortical tissue was reflected to expose the hippocampus. The left and right hippocampi were carefully isolated in their entirety, cleared of adhering cortical tissue and collected as bilateral hippocampal samples. The medial prefrontal cortex was dissected bilaterally from the anterior frontal cortex and comprised predominantly the prelimbic and infralimbic cortices, corresponding approximately to the + 3.2 to + 2.2 mm anterior-to-bregma region of the adult rat brain. Regional identification was guided by the stereotaxic anatomy described in the Paxinos and Watson rat brain atlas.

All dissections were performed rapidly on an ice-chilled surface using the same anatomical landmarks and dissection procedure for all animals. Collected tissues were immediately processed or frozen according to the requirements of the respective biochemical assays.

2.4 Determination of inflammatory cytokines

Tumour necrosis factor-α (TNF-α), interleukin-1β (IL-1β), and interleukin-6 (IL-6) were quantified in hippocampal and prefrontal cortical homogenates using rat-specific sandwich ELISA kits: Rat TNF-α Quantikine ELISA Kit (R&D Systems, Minneapolis, MN, USA; cat. no. RTA00), Rat IL-1β/IL-1F2 Quantikine ELISA Kit (cat. no. RLB00), and Rat IL-6 Quantikine ELISA Kit (cat. no. R6000B). Standards and samples were assayed in duplicate according to the manufacturer's instructions. Absorbance was measured at 450 nm with wavelength correction at 540 nm using a GloMax® Discover Multimode Microplate Reader (model GM3000; Promega Corporation, Madison, WI, USA). Cytokine concentrations were determined from the respective standard curves, normalized to total protein content, and expressed as pg/mg protein.

2.5 NF-κB/NLRP3 inflammasome-associated proteins

NF-κB/NLRP3 inflammasome-associated proteins were quantified in hippocampal and prefrontal cortical lysates by ELISA. Separate tissue aliquots were homogenized on ice in lysis buffer containing protease and phosphatase inhibitors, centrifuged to remove insoluble material, and the resulting

supernatants were used for analysis. Total protein concentration was determined using the bicinchoninic acid assay.

Total NF-κB p65 was quantified using a rat-specific quantitative sandwich ELISA kit (MyBioSource, San Diego, CA, USA; cat. no. MBS163007), while phosphorylation of NF-κB p65 at Ser536 was determined using a phospho-specific NF-κB p65 (Ser536) sandwich ELISA kit (MyBioSource; cat. no. MBS9511033). The latter uses phosphorylation-site-specific recognition of p65 phosphorylated at Ser536 and is reactive with rat samples. NLRP3 was quantified using the Rat NLRP3 SimpleStep ELISA Kit (Abcam, Cambridge, UK; cat. no. ab277086), a quantitative sandwich assay validated for rat tissue extracts. ASC/PYCARD was measured using the Rat Apoptosis-Associated Speck-Like Protein Containing a CARD (PYCARD) ELISA Kit (MyBioSource; cat. no. MBS9367701), which is suitable for rat tissue homogenates. Cleaved caspase-1 was quantified using a cleavage-specific Rat Cleaved-Caspase-1 ELISA Kit (MyBioSource; cat. no. MBS7255117), a quantitative competitive immunoassay validated for rat tissue homogenates.

Samples were assayed in duplicate according to the respective manufacturers' instructions, and absorbance was measured at 450 nm using a microplate reader. Analyte concentrations were determined from the corresponding standard curves and corrected for sample dilution. For each animal, total NF-κB p65, NLRP3, ASC and cleaved caspase-1 values were normalized to total protein content before statistical analysis. NF-κB p65 phosphorylation was expressed as the p-NF-κB p65 (Ser536)/total NF-κB p65 ratio, calculated individually for each animal. For graphical presentation of NLRP3, ASC and cleaved caspase-1, protein-normalized values were additionally expressed as fold change relative to the mean Control value, which was set to 1.0.

2.6 BDNF and synaptic plasticity-related proteins

Brain-derived neurotrophic factor (BDNF), synaptophysin, postsynaptic density protein-95 (PSD-95), and the N-methyl-D-aspartate receptor subunits NMDAR1, NMDAR2A and NMDAR2B were quantified separately in hippocampal and prefrontal cortical homogenates using rat-specific ELISA kits. Tissue samples were homogenized on ice in 50 mM phosphate buffer (pH 7.4) containing 1 mM EDTA and protease inhibitor cocktail at a tissue-to-buffer ratio of 1:10 (w/v), followed by centrifugation at 10,000 × g for 10 min at 4°C. The resulting supernatants were collected for analysis, and total protein concentration was determined using the Bradford protein assay.

BDNF was quantified using the Total BDNF Quantikine ELISA Kit validated for rat samples (R&D Systems, Minneapolis, MN, USA; cat. no. DBNT00). Synaptophysin, PSD-95 and NMDA receptor subunits were measured using rat-specific ELISA kits from Cloud-Clone Corp. (Wuhan, China): Synaptophysin/SYP ELISA Kit (cat. no. CEA425Ra), PSD-95/DLG4 ELISA Kit (cat. no. SEG168Ra), NMDAR1/GRIN1 ELISA Kit (cat. no. SEE805Ra), NMDAR2A/GRIN2A ELISA Kit (cat. no. SEE806Ra), and NMDAR2B/GRIN2B ELISA Kit (cat. no. SEE807Ra). All assays were performed according to the respective manufacturers’ instructions, with standards and samples assayed in duplicate. Absorbance was measured at 450 nm using a microplate reader, and analyte concentrations were calculated from the corresponding standard curves after correction for sample dilution.

BDNF concentrations were normalized to the total protein content of each tissue homogenate and expressed as pg/mg protein. For synaptophysin, PSD-95, NMDAR1, NMDAR2A and NMDAR2B, ELISA-derived concentrations were first normalized to total protein content for each animal. The normalized value for each animal was subsequently divided by the mean normalized value of the corresponding Control group within the same brain region. Results were therefore expressed as relative protein abundance (fold of Control), with the mean Control value set to 1.0.

2.7 Protein determination

Total protein concentration was determined according to the tissue-preparation workflow used for each analysis. For homogenates prepared for cytokine, BDNF and synaptic protein measurements, total protein concentration was determined using the Bradford protein assay. For lysates prepared separately for NF-κB/NLRP3 inflammasome-associated protein measurements, total protein concentration was determined using the bicinchoninic acid (BCA) assay. Measured analyte concentrations were normalized to the corresponding total protein concentration for each individual animal where applicable.

2.8 Statistical analysis

Statistical analyses were performed using GraphPad Prism version 10.4.1 for Windows (GraphPad Software, Boston, MA, USA). Data are presented as mean ± standard deviation (SD), with eight animals per group (n = 8/group). Normality was assessed using the Shapiro–Wilk test and inspection of Q–Q plots, and homogeneity of variance using the Brown–Forsythe test. Differences among the four experimental groups were evaluated using one-way analysis of variance (ANOVA) followed by Tukey's multiple-comparison test. Morris water maze escape latency across the four acquisition days was analysed using two-way repeated-measures ANOVA, with treatment group as the between-subject factor and training day as the within-subject factor. The main effects of treatment and training day and the treatment × training-day interaction were evaluated. Where appropriate, post-hoc comparisons between treatment groups at individual training days were performed with adjustment for multiple comparisons. Novel object recognition, Y-maze and open-field outcomes, together with cytokine, NF-κB/NLRP3-associated, BDNF and synaptic protein measurements, were analysed using one-way ANOVA followed by Tukey's multiple-comparison test. Hippocampal and prefrontal cortical outcomes were analysed separately. All tests were two-sided, and statistical significance was accepted at $p < 0.05$. In figures and tables, * denotes $p < 0.05$ versus Control, whereas # denotes $p < 0.05$ versus $CdCl_2$.

3. Results

3.1 DMF attenuated $CdCl_2$-associated behavioural impairments

Morris water maze performance improved across the four acquisition days in all groups, but the decline in escape latency was slower after $CdCl_2$ exposure. By Day 4, $CdCl_2$-treated rats showed a significantly longer escape latency than Control rats, whereas DMF co-treatment significantly reduced latency relative

to $CdCl_2$ alone; DMF alone remained comparable with Control (Fig. 1A, B). The available Day-4 post-hoc comparison did not support a significant residual difference between the $CdCl_2$+DMF and Control groups.

$CdCl_2$ also impaired novel-object recognition, with significant reductions in both recognition and discrimination indices compared with Control. DMF co-treatment significantly improved both recognition and discrimination indices relative to $CdCl_2$ alone. The recognition index remained significantly lower than Control, whereas the discrimination index did not differ significantly from Control; DMF alone remained comparable with Control (Fig. 1C, D).

In the Y-maze, $CdCl_2$ significantly reduced spontaneous alternation, while DMF co-treatment significantly improved performance relative to $CdCl_2$ alone, although values remained below Control (Fig. 1E). Total arm entries followed a similar pattern (Fig. 1F). Because $CdCl_2$ also reduced overall arm-entry activity, the spontaneous-alternation findings should be interpreted alongside the accompanying reduction in exploratory activity.

Consistent with this reduction in activity, $CdCl_2$ significantly decreased both rearing frequency and line crossings in the open-field test. DMF co-treatment significantly increased both measures relative to $CdCl_2$ alone, although values remained lower than Control, while DMF alone remained comparable with Control (Fig. 1G,H). Collectively, these findings indicate that DMF attenuated the $CdCl_2$-associated impairments across learning, recognition, spontaneous alternation and exploratory behaviour, while the accompanying reduction in locomotor activity should be considered when interpreting the cognitive endpoints.

3.2 DMF attenuated $CdCl_2$-induced increases in pro-inflammatory cytokines in the hippocampus and prefrontal cortex

$CdCl_2$ exposure markedly increased the concentrations of the pro-inflammatory cytokines TNF-α, IL-1β and IL-6 in both the hippocampus and prefrontal cortex (Fig. 2). Hippocampal TNF-α increased from 35.0 ± 2.5 pg/mg protein in Control animals to 89.5 ± 5.5 pg/mg protein following $CdCl_2$ exposure ($p < 0.05$). DMF alone produced a value of 31.5 ± 2.5 pg/mg protein, whereas DMF co-treatment reduced TNF-α in $CdCl_2$-exposed animals to 51.0 ± 3.5 pg/mg protein ($p < 0.05$ vs $CdCl_2$), although the level remained higher than Control ($p < 0.05$). A similar response was observed in the prefrontal cortex, where TNF-α increased from 30.5 ± 2.3 pg/mg protein in Control animals to 76.5 ± 5.0 pg/mg protein in the $CdCl_2$ group ($p < 0.05$). Co-treatment with DMF reduced this value to 44.5 ± 3.2 pg/mg protein ($p < 0.05$ vs $CdCl_2$), while DMF alone remained comparable with Control at 28.5 ± 2.2 pg/mg protein.

Hippocampal IL-1β similarly increased from 18.0 ± 1.5 pg/mg protein in Control animals to 56.0 ± 4.0 pg/mg protein following $CdCl_2$ exposure ($p < 0.05$). DMF alone produced 17.0 ± 2.0 pg/mg protein, while $CdCl_2$+DMF treatment reduced IL-1β to 31.0 ± 2.8 pg/mg protein ($p < 0.05$ vs $CdCl_2$), although it remained above Control ($p < 0.05$). In the prefrontal cortex, IL-1β increased from 16.0 ± 1.5 pg/mg protein in

Control animals to 49.5 ± 3.5 pg/mg protein after $CdCl_2$ exposure ($p < 0.05$). DMF alone yielded 15.0 ± 1.5 pg/mg protein, whereas DMF co-treatment reduced the $CdCl_2$-associated increase to 27.0 ± 2.5 pg/mg protein ($p < 0.05$ vs $CdCl_2$; $p < 0.05$ vs Control).

The same pattern was evident for IL-6. Hippocampal IL-6 increased from 24.5 ± 2.0 pg/mg protein in Control animals to 72.0 ± 5.0 pg/mg protein following $CdCl_2$ exposure ($p < 0.05$). DMF alone produced 22.0 ± 1.8 pg/mg protein, whereas $CdCl_2$+DMF treatment reduced IL-6 to 41.0 ± 3.0 pg/mg protein ($p < 0.05$ vs $CdCl_2$), although levels remained above Control ($p < 0.05$). In the prefrontal cortex, IL-6 increased from 21.0 ± 2.0 pg/mg protein in Control animals to 64.0 ± 4.5 pg/mg protein following $CdCl_2$ exposure ($p < 0.05$). DMF alone yielded 20.0 ± 1.5 pg/mg protein, while DMF co-treatment reduced IL-6 to 36.0 ± 3.0 pg/mg protein ($p < 0.05$ vs $CdCl_2$; $p < 0.05$ vs Control). Collectively, these findings show that $CdCl_2$ elicited a consistent pro-inflammatory response in both brain regions, which was substantially attenuated, although not completely normalized, by DMF.

3.3 DMF attenuated $CdCl_2$-associated increases in NF-κB/NLRP3 inflammasome-associated signalling

$CdCl_2$ exposure markedly increased NF-κB p65 protein expression in both brain regions. In the hippocampus, NF-κB p65 increased from 1.00 ± 0.08-fold in Control animals to 2.80 ± 0.20-fold following $CdCl_2$ exposure ($p < 0.05$). DMF alone remained close to Control (0.90 ± 0.08-fold), whereas DMF co-treatment reduced NF-κB p65 expression in $CdCl_2$-exposed animals to 1.52 ± 0.12-fold ($p < 0.05$ vs $CdCl_2$), although it remained above Control ($p < 0.05$). A similar pattern was observed in the prefrontal cortex, where NF-κB p65 increased from 1.00 ± 0.07-fold in Control animals to 2.52 ± 0.17-fold after $CdCl_2$ exposure. DMF alone produced 0.95 ± 0.06-fold, while $CdCl_2$+DMF reduced expression to 1.40 ± 0.11-fold ($p < 0.05$ vs $CdCl_2$).

The p-NF-κB p65/NF-κB p65 ratio showed a corresponding increase following $CdCl_2$ exposure. In the hippocampus, the phosphorylation ratio increased from 0.38 ± 0.04 in Control animals to 1.21 ± 0.09 in the $CdCl_2$ group ($p < 0.05$). DMF alone produced 0.34 ± 0.03, whereas co-treatment reduced the ratio to 0.63 ± 0.05 ($p < 0.05$ vs $CdCl_2$). In the prefrontal cortex, the ratio similarly increased from 0.35 ± 0.03 to 1.07 ± 0.08 following $CdCl_2$ exposure and was reduced to 0.57 ± 0.04 by DMF co-treatment. DMF alone remained comparable with Control (0.32 ± 0.02).

Consistent with NF-κB activation, NLRP3 protein expression was substantially elevated by $CdCl_2$. Hippocampal NLRP3 increased from 1.00 ± 0.08-fold in Control animals to 3.10 ± 0.22-fold following $CdCl_2$ exposure ($p < 0.05$). DMF alone produced 0.90 ± 0.07-fold, whereas DMF co-treatment reduced NLRP3 to 1.62 ± 0.13-fold ($p < 0.05$ vs $CdCl_2$). In the prefrontal cortex, $CdCl_2$ increased NLRP3 from 1.00 ± 0.07-fold to 2.78 ± 0.20-fold, while DMF co-treatment reduced expression to 1.48 ± 0.12-fold. DMF alone remained close to Control (0.90 ± 0.06-fold).

A similar treatment pattern was observed for ASC. In the hippocampus, ASC expression increased from 1.00 ± 0.08-fold in Control animals to 2.65 ± 0.18-fold following $CdCl_2$ exposure ($p < 0.05$). DMF alone

produced 0.92 ± 0.07-fold, whereas $CdCl_2$+DMF reduced ASC expression to 1.43 ± 0.11-fold ($p < 0.05$ vs $CdCl_2$). In the prefrontal cortex, ASC increased from 1.00 ± 0.06-fold to 2.38 ± 0.16-fold after $CdCl_2$ exposure and was reduced to 1.33 ± 0.10-fold by DMF co-treatment; DMF alone remained comparable with Control (0.95 ± 0.06-fold).

Finally, cleaved caspase-1 was markedly increased following $CdCl_2$ exposure, consistent with activation of inflammasome-associated inflammatory signalling. Hippocampal cleaved caspase-1 increased from 1.00 ± 0.08-fold in Control animals to 2.92 ± 0.21-fold in the $CdCl_2$ group ($p < 0.05$). DMF alone produced 0.88 ± 0.06-fold, whereas co-treatment reduced cleaved caspase-1 to 1.54 ± 0.12-fold ($p < 0.05$ vs $CdCl_2$). In the prefrontal cortex, $CdCl_2$ increased cleaved caspase-1 from 1.00 ± 0.07-fold to 2.60 ± 0.18-fold, while DMF co-treatment reduced it to 1.42 ± 0.11-fold. DMF alone remained comparable with Control (0.92 ± 0.06-fold).

Overall, $CdCl_2$ produced coordinated increases in NF-κB expression and phosphorylation together with increased NLRP3, ASC and cleaved caspase-1 in both the hippocampus and prefrontal cortex. DMF substantially attenuated these changes, although most measures remained above Control levels, indicating attenuation of $CdCl_2$-associated NF-κB/NLRP3 inflammasome-associated signalling.

3.4 DMF attenuated $CdCl_2$-induced reductions in BDNF and synaptic plasticity-related proteins

$CdCl_2$ exposure significantly reduced BDNF, synaptophysin, PSD-95, NMDAR1, NMDAR2A and NMDAR2B in both the hippocampus and prefrontal cortex compared with Control ($p < 0.05$; Table 1). DMF administered alone did not differ significantly from Control for any of these endpoints. In $CdCl_2$-exposed rats, DMF co-treatment significantly increased all measured neurotrophic and synaptic plasticity-related proteins relative to $CdCl_2$ alone ($p < 0.05$), although the extent of recovery differed among proteins and brain regions.

In the hippocampus, BDNF, synaptophysin, NMDAR1 and NMDAR2A in the $CdCl_2$+DMF group no longer differed significantly from Control, whereas PSD-95 and NMDAR2B remained significantly reduced despite improvement relative to $CdCl_2$ alone ($p < 0.05$; Table 1). In the prefrontal cortex, BDNF, synaptophysin, NMDAR1, NMDAR2A and NMDAR2B in the co-treatment group did not differ significantly from Control; however, PSD-95 remained significantly lower than Control despite its significant increase relative to $CdCl_2$ alone.

Overall, these findings demonstrate that DMF substantially attenuated the $CdCl_2$-associated reductions in neurotrophic and synaptic plasticity-related proteins, but recovery was endpoint dependent rather than complete, with persistent reductions in hippocampal PSD-95 and NMDAR2B and prefrontal cortical PSD-95.

Table 1

Effects of $CdCl_2$ and dimethyl fumarate (DMF) on BDNF and synaptic plasticity-related proteins in the hippocampus and prefrontal cortex. Data are presented as mean ± SD (n = 8 rats/group). Statistical comparisons were performed using one-way ANOVA followed by Tukey's multiple-comparison test. $^{*}p < 0.05$ versus Control; $^{\#}p < 0.05$ versus $CdCl_2$. Values marked $^{*\#}$ differed significantly from both Control and $CdCl_2$.

Endpoint	Unit	Control	$CdCl_2$	DMF	$CdCl_2$ + DMF
BDNF (hippocampus)	pg/mg protein	91.23 ± 16.86	44.91 ± 10.92*	97.54 ± 17.88$^{\#}$	75.09 ± 14.88$^{\#}$
Synaptophysin (hippocampus)	fold of control	0.99 ± 0.20	0.46 ± 0.14*	1.04 ± 0.23$^{\#}$	0.75 ± 0.17$^{\#}$
PSD-95 (hippocampus)	fold of control	0.99 ± 0.20	0.41 ± 0.11*	1.07 ± 0.25$^{\#}$	0.72 ± 0.17$^{*\#}$
NMDAR1 (hippocampus)	fold of control	1.00 ± 0.17	0.51 ± 0.14*	1.02 ± 0.20$^{\#}$	0.80 ± 0.17$^{\#}$
NMDAR2A (hippocampus)	fold of control	0.99 ± 0.17	0.48 ± 0.11*	1.03 ± 0.20$^{\#}$	0.77 ± 0.17$^{\#}$
NMDAR2B (hippocampus)	fold of control	0.99 ± 0.20	0.44 ± 0.11*	1.05 ± 0.23$^{\#}$	0.74 ± 0.17$^{*\#}$
BDNF (prefrontal cortex)	pg/mg protein	83.63 ± 14.88	40.94 ± 9.93*	88.30 ± 16.55$^{\#}$	69.01 ± 13.24$^{\#}$
Synaptophysin (prefrontal cortex)	fold of control	0.99 ± 0.17	0.50 ± 0.14*	1.02 ± 0.20$^{\#}$	0.79 ± 0.17$^{\#}$
PSD-95 (prefrontal cortex)	fold of control	1.00 ± 0.17	0.45 ± 0.11*	1.04 ± 0.20$^{\#}$	0.76 ± 0.17$^{*\#}$
NMDAR1 (prefrontal cortex)	fold of control	1.00 ± 0.17	0.55 ± 0.14*	1.00 ± 0.17$^{\#}$	0.83 ± 0.17$^{\#}$
NMDAR2A (prefrontal cortex)	fold of control	0.99 ± 0.17	0.52 ± 0.11*	1.01 ± 0.17$^{\#}$	0.80 ± 0.17$^{\#}$
NMDAR2B (prefrontal cortex)	fold of control	0.99 ± 0.17	0.49 ± 0.14*	1.02 ± 0.20$^{\#}$	0.77 ± 0.17$^{\#}$

4. Discussion

The present study provides convergent evidence that $CdCl_2$ exposure disrupts behavioural function while promoting inflammatory and synaptic alterations in the hippocampus and prefrontal cortex, and that DMF substantially attenuates this pattern of injury. The importance of the findings lies less in any single

marker than in their consistency across functional and molecular levels. $CdCl_2$-induced deficits in spatial learning, recognition memory, spontaneous alternation and exploratory behaviour occurred alongside increased pro-inflammatory cytokines, enhanced NF-κB/NLRP3 inflammasome-associated signalling, and reductions in proteins involved in neurotrophic support and synaptic organization. DMF shifted each of these domains toward the control phenotype, although recovery was incomplete for several endpoints. This coordinated response supports a neuroprotective effect of DMF in this model, while also indicating that its behavioural benefits are associated with, rather than proven to result directly from, suppression of inflammatory signalling.

The behavioural findings are consistent with previous evidence that Cd exposure compromises cognition. Experimental studies have reported impaired hippocampus-dependent learning and memory, reduced neurogenesis and structural neuronal injury following Cd exposure (Wang et al., 2019; El-Kott et al., 2020). Ali et al. (2021) similarly observed impaired Morris water maze and Y-maze performance in Cd-exposed mice, accompanied by synaptic abnormalities in hippocampal and cortical tissue. More recent findings by Nasir et al. (2025) also linked Cd exposure with memory impairment, neuroinflammatory signalling and disruption of synaptic proteins. The present findings extend this pattern by showing concordant abnormalities across several behavioural domains, including spatial acquisition, object recognition, spontaneous alternation and exploratory activity. Importantly, DMF improved performance across these tests rather than affecting a single behavioural endpoint. Such consistency strengthens the interpretation that DMF produced a meaningful functional benefit.

The behavioural data nevertheless require careful interpretation. $CdCl_2$ also reduced total arm entries, rearing frequency and line crossings, indicating a substantial decline in exploratory or locomotor activity. Reduced activity could influence performance in tasks such as the Y-maze and novel object recognition test and therefore should not be ignored when attributing poorer performance exclusively to memory dysfunction. Similarly, escape latency in the Morris water maze can be influenced by swimming ability or general motor performance if swimming speed is not independently assessed. For this reason, the present findings are more accurately described as a combination of cognitive and behavioural impairment rather than evidence of isolated memory loss. Even with this qualification, the convergence of findings across tasks that rely on different behavioural demands supports a genuine disturbance of neural function after Cd exposure.

The improvement produced by DMF is broadly consistent with observations in other neuroinflammatory models. Paraiso et al. (2018) reported that DMF reduced microglial inflammatory activity and improved novel-object recognition following systemic inflammatory challenge. Yan et al. (2021) similarly found that DMF improved cognitive performance in chronic cerebral hypoperfusion while reducing oxidative and inflammatory signalling. In an Alzheimer-type model, Wang et al. (2024) also reported reduced neuroinflammation and improved cognitive performance after DMF treatment. Although these models differ substantially from Cd toxicity, they provide independent evidence that the behavioural effects of DMF can accompany suppression of neuroinflammatory responses. The present study therefore adds

environmental metal neurotoxicity to the experimental settings in which DMF has shown neurobehavioural benefit.

A particularly consistent feature of the present study was the inflammatory response in both brain regions. $CdCl_2$ increased TNF-α, IL-1β and IL-6 in the hippocampus and prefrontal cortex, while DMF substantially reduced these elevations. These findings agree with earlier reports that Cd can induce a pro-inflammatory environment in neural tissue. El-Kott et al. (2020), for example, associated Cd-induced hippocampal injury with increased inflammatory cytokines and NF-κB activation. The present findings are notable because the cytokine response was accompanied by corresponding changes in NF-κB p65 expression and its phosphorylation state, providing a plausible signalling context for the inflammatory phenotype.

NF-κB is a central regulator of inflammatory gene expression, but the present results should not be interpreted as evidence that NF-κB alone mediated the effects of Cd or DMF. Rather, the increase in NF-κB p65 and the p-NF-κB p65/NF-κB p65 ratio after $CdCl_2$ exposure, together with their reduction following DMF treatment, is consistent with altered NF-κB-associated inflammatory signalling. This interpretation is supported by Gillard et al. (2015), who showed that DMF can inhibit NF-κB activity under experimental inflammatory conditions, and by Paraiso et al. (2018), who linked DMF treatment with reduced NF-κB activation in microglia. Nevertheless, measurements of total and phosphorylated NF-κB do not establish transcriptional activity as directly as nuclear translocation, DNA-binding assays or pathway-specific inhibition would. Accordingly, the present data support attenuation of NF-κB-associated signalling, rather than definitive demonstration that inhibition of NF-κB was required for the protective effect of DMF.

The NLRP3-related findings provide an additional layer to this inflammatory response. $CdCl_2$ increased NLRP3, ASC and cleaved caspase-1 in both the hippocampus and prefrontal cortex, whereas DMF substantially attenuated these changes. The simultaneous increase in these components, particularly in the presence of elevated IL-1β, is consistent with enhanced NLRP3 inflammasome-associated signalling. This agrees with Cai et al. (2021), who demonstrated increased NLRP3, ASC and caspase-1 following Cd exposure and proposed interaction between NF-κB signalling and inflammasome activation. Wang et al. (2023) likewise linked Cd-induced cognitive dysfunction with NLRP3 inflammasome-related responses involving mitochondrial oxidative stress, while Zhu et al. (2026) recently reported behavioural impairment and NLRP3-associated neuronal injury after Cd exposure.

The ability of DMF to reduce NLRP3, ASC and cleaved caspase-1 is also supported by previous mechanistic studies. Tastan et al. (2021) demonstrated that DMF suppressed microglial NLRP3 inflammasome activation, reduced caspase-1 and inflammatory cytokines and improved inflammation-related behaviour in mice. More recently, Hu et al. (2024) reported that DMF can covalently modify NLRP3 at Cys673 and interfere with inflammasome activation. These findings provide biological plausibility for the reduction observed in the present study. However, they do not justify concluding that the same direct molecular interaction occurred in the present Cd model. No selective NLRP3 inhibitor,

genetic manipulation or direct assay of NLRP3 modification was included. The appropriate interpretation is therefore that DMF-mediated protection occurred in association with reduced NLRP3 inflammasome-associated signalling.

A similar caution applies to pyroptosis. Increased NLRP3, ASC and cleaved caspase-1 is compatible with inflammasome activation, but it is insufficient on its own to establish pyroptotic cell death. Direct evidence of pyroptosis would require additional endpoints such as gasdermin-D cleavage, membrane pore formation, LDH release or cell-specific evidence of pyroptotic morphology. Although Wang et al. (2023) and Zhu et al. (2026) demonstrated pyroptosis-related mechanisms in their respective Cd models, those observations should support the biological interpretation of the present findings rather than be taken as evidence that pyroptosis was directly demonstrated here.

The inflammatory changes were accompanied by substantial reductions in BDNF and several proteins associated with synaptic organization and glutamatergic signalling.

The reduction in BDNF and synaptic plasticity-related proteins provides a plausible molecular link between this inflammatory environment and impaired behavioural function. $CdCl_2$ decreased BDNF, synaptophysin, PSD-95 and NMDA receptor subunits in both the hippocampus and prefrontal cortex, while DMF restored these proteins to varying degrees. This pattern agrees with previous evidence that Cd can disrupt proteins required for synaptic organization and signalling. Ali et al. (2021) reported reductions in synaptophysin and PSD-95 after chronic Cd exposure, while Yang et al. (2023) observed abnormalities in glutamate receptor-associated proteins together with synaptic and glial changes. The reduction in BDNF is also consistent with Batool et al. (2022), who linked Cd-associated cognitive dysfunction with reduced hippocampal BDNF.

The partial restoration of these proteins by DMF is particularly relevant to the behavioural findings. BDNF supports neuronal survival and activity-dependent plasticity; synaptophysin is associated with presynaptic vesicle organization; PSD-95 contributes to postsynaptic architecture; and NMDA receptor subunits are integral to glutamatergic signalling underlying learning-related synaptic modification. Restoration of these proteins therefore provides a plausible molecular context for the improvement in learning and memory-related performance. However, protein abundance should not be equated directly with synaptic function. Neither synaptic transmission nor long-term potentiation was measured electrophysiologically. The findings are therefore best described as preservation of synaptic plasticity-related proteins or molecular indices of synaptic integrity, rather than direct restoration of synaptic plasticity itself.

It is also noteworthy that DMF did not normalize every endpoint completely. Hippocampal PSD-95 and NMDAR2B, as well as prefrontal PSD-95, remained significantly altered relative to Control despite substantial improvement relative to $CdCl_2$ alone. This incomplete recovery is biologically informative. It suggests that different components of the synaptic machinery may have different sensitivities to Cd injury or different capacities for recovery during DMF treatment. It also argues against portraying DMF as completely reversing Cd neurotoxicity. The more defensible conclusion is that DMF substantially

attenuated the injury while leaving residual abnormalities in selected molecular and behavioural endpoints.

Viewed together, the findings support an integrated model in which Cd exposure is associated with behavioural impairment occurring in parallel with inflammatory activation and loss of neurotrophic and synaptic proteins. DMF substantially attenuated these changes, and the mechanistic relationships integrating the principal molecular and functional findings are summarized in Fig. 4. The strength of the study lies in this convergence across two cognition-relevant brain regions and across behavioural, inflammatory and synaptic domains. Nevertheless, the data should not be arranged into a fixed causal sequence in which Cd activates NF-κB, which then activates NLRP3 and subsequently causes synaptic disruption and behavioural impairment. Such a pathway is biologically plausible and supported by previous mechanistic studies, but it was not experimentally dissected here. Demonstrating pathway dependence would require interventions such as selective NF-κB or NLRP3 inhibition, genetic manipulation or formal mediation approaches.

Several limitations therefore deserve consideration. First, the study establishes associations between DMF treatment, reduced inflammatory signalling and improved behavioural performance but does not determine which molecular pathway is necessary for protection. Second, the cellular origin of the measured inflammatory proteins was not established. Third, the inflammasome measurements support NLRP3-associated signalling but do not directly demonstrate inflammasome assembly or pyroptotic cell death. Fourth, synaptic protein measurements provide molecular evidence of altered synaptic integrity but do not substitute for electrophysiological assessment of synaptic transmission or plasticity. Finally, the reduction in exploratory and locomotor activity after $CdCl_2$ exposure may have contributed to performance in some behavioural tasks and should be considered when interpreting cognitive outcomes. In addition, only male rats were studied; therefore, potential sex-related differences in the neurotoxic effects of $CdCl_2$ or the response to DMF were not assessed.

Within these limitations, the present study provides evidence that DMF substantially attenuates $CdCl_2$-induced neurobehavioural dysfunction and is associated with reduced pro-inflammatory cytokine production, reduced NF-κB/NLRP3 inflammasome-associated signalling, and preservation of BDNF and key synaptic proteins in the hippocampus and prefrontal cortex. Rather than supporting a single isolated mechanism, the findings suggest that DMF protection involves coordinated modulation of inflammatory and synaptic disturbances produced by Cd exposure. Direct pathway-intervention studies will be required to determine whether suppression of NF-κB/NLRP3 signalling is necessary for the neuroprotective effect of DMF.

Abbreviations

3Rs – Replacement, Reduction and Refinement

ANOVA – Analysis of variance

ARRIVE – Animal Research: Reporting of In Vivo Experiments

ASC – Apoptosis-associated speck-like protein containing a CARD

BCA – Bicinchoninic acid

BDNF – Brain-derived neurotrophic factor

CARD – Caspase activation and recruitment domain

Cd – Cadmium

$CdCl_2$ – Cadmium chloride

CMC – Carboxymethylcellulose

DLG4 – Discs large membrane-associated guanylate kinase scaffold protein 4

DMF – Dimethyl fumarate

DNA – Deoxyribonucleic acid

EDTA – Ethylenediaminetetraacetic acid

ELISA – Enzyme-linked immunosorbent assay

GFAP – Glial fibrillary acidic protein

GRIN1 – Glutamate ionotropic receptor NMDA type subunit 1

GRIN2A – Glutamate ionotropic receptor NMDA type subunit 2A

GRIN2B – Glutamate ionotropic receptor NMDA type subunit 2B

Iba1 – Ionized calcium-binding adaptor molecule 1

IL-1β – Interleukin-1 beta

IL-1F2 – Interleukin-1 family member 2

IL-6 – Interleukin-6

i.p. – Intraperitoneal

IκB-α – Inhibitor of nuclear factor kappa-B alpha

LDH – Lactate dehydrogenase

NF-κB – Nuclear factor kappa-light-chain-enhancer of activated B cells

NMDA – N-Methyl-D-aspartate

NMDAR1 – N-Methyl-D-aspartate receptor subunit 1

NMDAR2A – N-Methyl-D-aspartate receptor subunit 2A

NMDAR2B – N-Methyl-D-aspartate receptor subunit 2B

NLRP3 – NLR family pyrin domain-containing protein 3

Nrf2/NRF2 – Nuclear factor erythroid 2-related factor 2

p-NF-κB – Phosphorylated nuclear factor kappa-B

PSD-95 – Postsynaptic density protein 95

PYCARD – Pyrin domain and CARD domain-containing protein

Q–Q – Quantile–quantile

SD – Standard deviation

SYP – Synaptophysin

TNF-α – Tumour necrosis factor alpha

Declarations

5.1 Funding: This research received no external funding and was supported by voluntary contributions from members of the research team.

5.2 Competing interests: All authors declare no known competing interest for this research.

5.3 Data availability: The datasets generated and analysed during the current study, including the underlying numerical data and supporting source data, are available from the corresponding author upon reasonable request.

5.4 CRediT authorship contribution statement

Samuel Bolaji Mesole: Conceptualization, Methodology, Investigation, Formal analysis, Data curation, Visualization, Writing – original draft.

Alfred Omachonu Okpanachi: Methodology, Investigation, Validation, Writing – review and editing.

Oria Sunday Rademene: Formal analysis, Validation and Data curation.

Yusuf Ademola Uthman: Methodology, Formal analysis, Validation, Writing – review and editing.

Kebe Edet Obeten: Investigation, Data curation.

Mwitwa Kombe: Resources, Writing – review and editing.

Sharon Kaundu: Investigation, Writing – review and editing.

Chinyama Jonathan: Methodology, Validation, Writing – review and editing.

Kafunda Tuesday: Formal analysis.

5.5 Declaration of generative AI and AI-assisted technologies in the manuscript preparation process

During the preparation of this work, the authors used ChatGPT, Grammarly and QuillBot for grammatical correction and language refinement. The authors reviewed and edited the outputs as needed and take full responsibility for the content of the manuscript.

References

Ali T, Khan A, Alam SI, Ahmad S, Ikram M, Park JS, Lee HJ, Kim MO. Cadmium, an environmental contaminant, exacerbates Alzheimer's pathology in the aged mice's brain. *Frontiers in Aging Neuroscience*. 2021;13:650930. doi:10.3389/fnagi.2021.650930.

Batool A, Saleem S, Naqvi F, Hasan KA, Naqvi F, Haider S. Thymol mitigates cadmium-induced behavioral and cognitive deficits by up-regulating hippocampal BDNF levels in rats. *Pakistan Journal of Pharmaceutical Sciences*. 2022;35(2 Special):671–678. doi:10.36721/PJPS.2022.35.2.SP.671-678.1.

Cai J, Guan H, Jiao X, Yang J, Chen X, Zhang H, et al. NLRP3 inflammasome mediated pyroptosis is involved in cadmium exposure-induced neuroinflammation through the IL-1β/IκB-α/NF-κB/NLRP3 feedback loop in swine. *Toxicology*. 2021;453:152720. doi:10.1016/j.tox.2021.152720.

Carlström KE, Chinthakindi PK, Espinosa B, Al Nimer F, Arnér ESJ, Arvidsson PI, Piehl F, Johansson K. Characterization of more selective central nervous system Nrf2-activating novel vinyl sulfoximine compounds compared to dimethyl fumarate. *Neurotherapeutics*. 2020;17(3):1142–1152. doi:10.1007/s13311-020-00855-0.

El-Kott AF, Alshehri AS, Khalifa HS, Abd-Lateif AEM, Alshehri MA, Abd El-Maksoud MMA, et al. Cadmium chloride induces memory deficits and hippocampal damage by activating the JNK/p66Shc/NADPH oxidase axis. *International Journal of Toxicology*. 2020;39(5):477–490. doi:10.1177/1091581820930651.

Gillard GO, Collette B, Anderson J, Chao J, Scannevin RH, Huss DJ, Fontenot JD. DMF, but not other fumarates, inhibits NF-κB activity in vitro in an Nrf2-independent manner. *Journal of Neuroimmunology*. 2015;283:74–85. doi:10.1016/j.jneuroim.2015.04.006.

Gök E, Deveci E. Histopathological evaluation of IBA-1, GFAP activity in the brain cortex of rats administered cadmium chloride. *Archives Italiennes de Biologie*. 2022;160(1–2):20–27. doi:10.12871/000398292022122.

Gustin K, Tofail F, Vahter M, Kippler M. Cadmium exposure and cognitive abilities and behavior at 10 years of age: a prospective cohort study. *Environment International*. 2018;113:259–268. doi:10.1016/j.envint.2018.02.020.

Han R, Xiao J, Zhai H, Hao J. Dimethyl fumarate attenuates experimental autoimmune neuritis through the nuclear factor erythroid-derived 2-related factor 2/heme oxygenase-1 pathway by altering the balance of M1/M2 macrophages. *Journal of Neuroinflammation*. 2016;13:97. doi:10.1186/s12974-016-0559-x.

Hu H, Cai Y, Shi Y, Zhang S, Yu X, Ma T, et al. Dimethyl fumarate covalently modifies Cys673 of NLRP3 to exert anti-inflammatory effects. *iScience*. 2024;27(4):109544. doi:10.1016/j.isci.2024.109544.

Nasir A, Rahman MU, Khan M, Zahid M, Shahab M, Jiao H, et al. Vitamin B6 via p-JNK/Nrf-2/NF-κB signaling ameliorates cadmium chloride-induced oxidative stress mediated memory deficits in mice hippocampus. *Current Neuropharmacology*. 2025;23(1):116–127. doi:10.2174/1570159X22999240730154422.

Oboh G, Adebayo AA, Ademosun AO, Olowokere OG. Rutin restores neurobehavioral deficits via alterations in cadmium bioavailability in the brain of rats exposed to cadmium. *NeuroToxicology*. 2020;77:12–19. doi:10.1016/j.neuro.2019.12.008.

Paraiso HC, Kuo PC, Curfman ET, Moon HJ, Sweazey RD, Yen JH, Chang FL, Yu IC. Dimethyl fumarate attenuates reactive microglia and long-term memory deficits following systemic immune challenge. *Journal of Neuroinflammation*. 2018;15:100. doi:10.1186/s12974-018-1125-5.

Tastan B, Arioz BI, Tufekci KU, Tarakcioglu E, Gonul CP, Genc K, Genc S. Dimethyl fumarate alleviates NLRP3 inflammasome activation in microglia and sickness behavior in LPS-challenged mice. *Frontiers in Immunology*. 2021;12:737065. doi:10.3389/fimmu.2021.737065.

Wang D, Wu Y, Sun S, Zhao P, Zhou X, et al. NLRP3 inflammasome-mediated pyroptosis involvement in cadmium exposure-induced cognitive deficits via the Sirt3-mtROS axis. *Science of the Total Environment*. 2023;903:166478. doi:10.1016/j.scitotenv.2023.166478.

Wang H, Abel GM, Storm DR, Xia Z. Cadmium exposure impairs adult hippocampal neurogenesis. *Toxicological Sciences*. 2019;171(2):501–514. doi:10.1093/toxsci/kfz152.

Wang T, Sobue A, Watanabe S, Komine O, Saido TC, Saito T, Yamanaka K. Dimethyl fumarate improves cognitive impairment and neuroinflammation in mice with Alzheimer's disease. *Journal of Neuroinflammation*. 2024;21:55. doi:10.1186/s12974-024-03046-2.

Wilms H, Sievers J, Rickert U, Rostami-Yazdi M, Mrowietz U, Lucius R. Dimethylfumarate inhibits microglial and astrocytic inflammation by suppressing the synthesis of nitric oxide, IL-1β, TNF-α and IL-6 in an in-vitro model of brain inflammation. *Journal of Neuroinflammation*. 2010;7:30. doi:10.1186/1742-2094-7-30.

Yan N, Xu Z, Qu C, Zhang J. Dimethyl fumarate improves cognitive deficits in chronic cerebral hypoperfusion rats by alleviating inflammation, oxidative stress, and ferroptosis via NRF2/ARE/NF-κB signal pathway. *International Immunopharmacology*. 2021;98:107844. doi:10.1016/j.intimp.2021.107844.

Yang JY, Wang J, Hu Y, Shen DY, Xiao GL, Qin XY, Lan R. Paeoniflorin improves cognitive dysfunction, restores glutamate receptors, attenuates gliosis and maintains synaptic plasticity in cadmium-intoxicated mice. *Arabian Journal of Chemistry*. 2023;16(1):104406. doi:10.1016/j.arabjc.2022.104406.

Zhu Y, Yuan Q, Geng J, Hu J, Zhao P, Yan Y, et al. Ameliorative effects of urolithin A against cadmium-induced NLRP3-mediated pyroptosis and cognitive deficits via regulating aryl hydrocarbon receptor signaling. *Biological Trace Element Research*. 2026;204:2806–2821. doi:10.1007/s12011-025-04858-w.

Figures

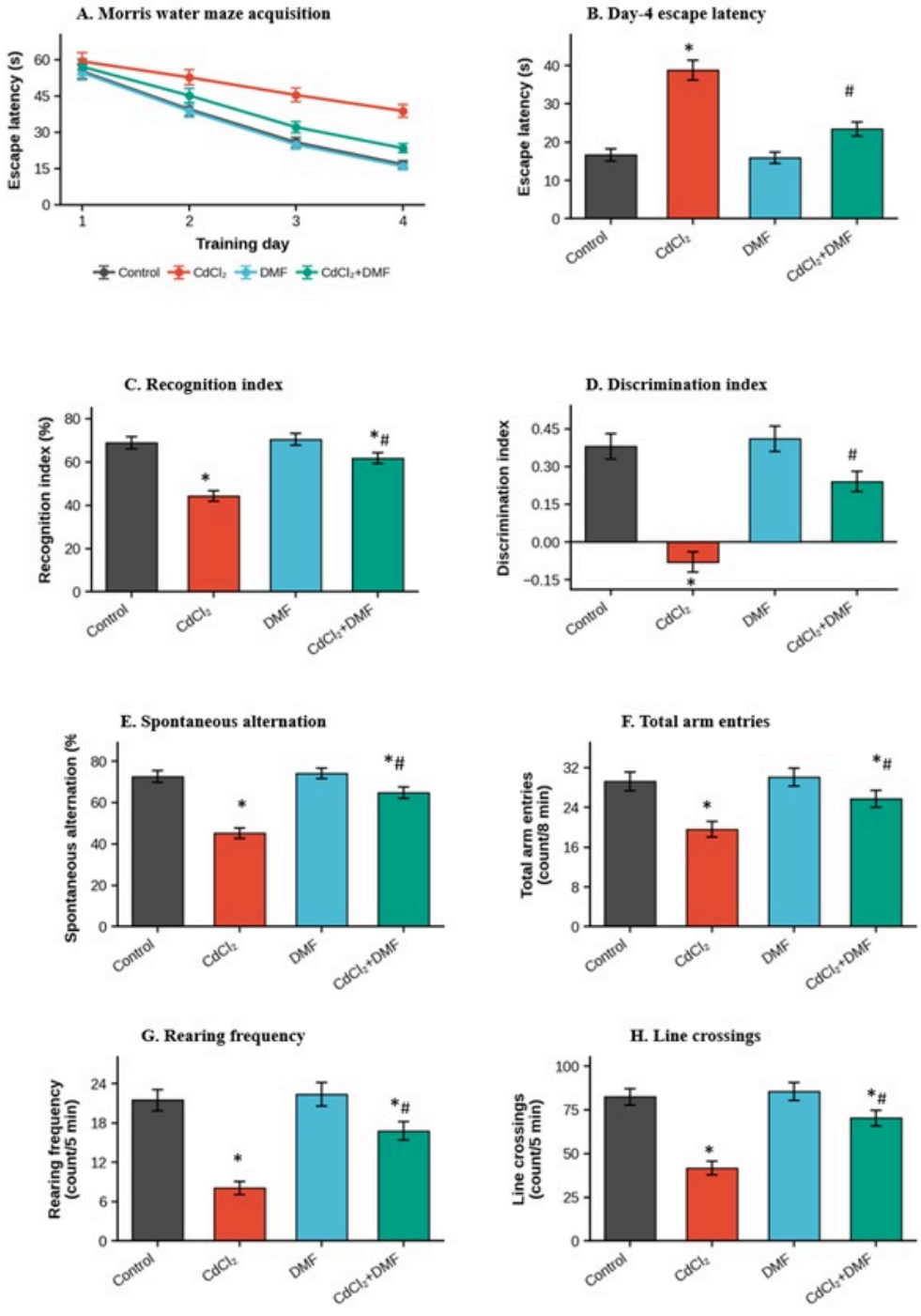


Figure 1

Effects of dimethyl fumarate on $CdCl_2$-induced alterations in learning, memory and exploratory behaviour.

(A) Morris water maze escape latency across four acquisition days; (B) escape latency on acquisition Day 4; (C) novel object recognition index; (D) novel object discrimination index; (E) Y-maze spontaneous

alternation; (F) total Y-maze arm entries; (G) open-field rearing frequency; and (H) open-field line crossings. Data are presented as mean ± SD (n = 8 rats/group) for Control, $CdCl_2$, DMF and $CdCl_2$+DMF groups. Morris water maze acquisition data were analysed using two-way repeated-measures ANOVA with treatment group as the between-subject factor and training day as the within-subject factor, followed where appropriate by multiplicity-adjusted post-hoc comparisons. Novel object recognition, Y-maze and open-field outcomes were analysed using one-way ANOVA followed by Tukey's multiple-comparison test. *p < 0.05 versus Control; #p < 0.05 versus $CdCl_2$. $CdCl_2$, cadmium chloride; DMF, dimethyl fumarate

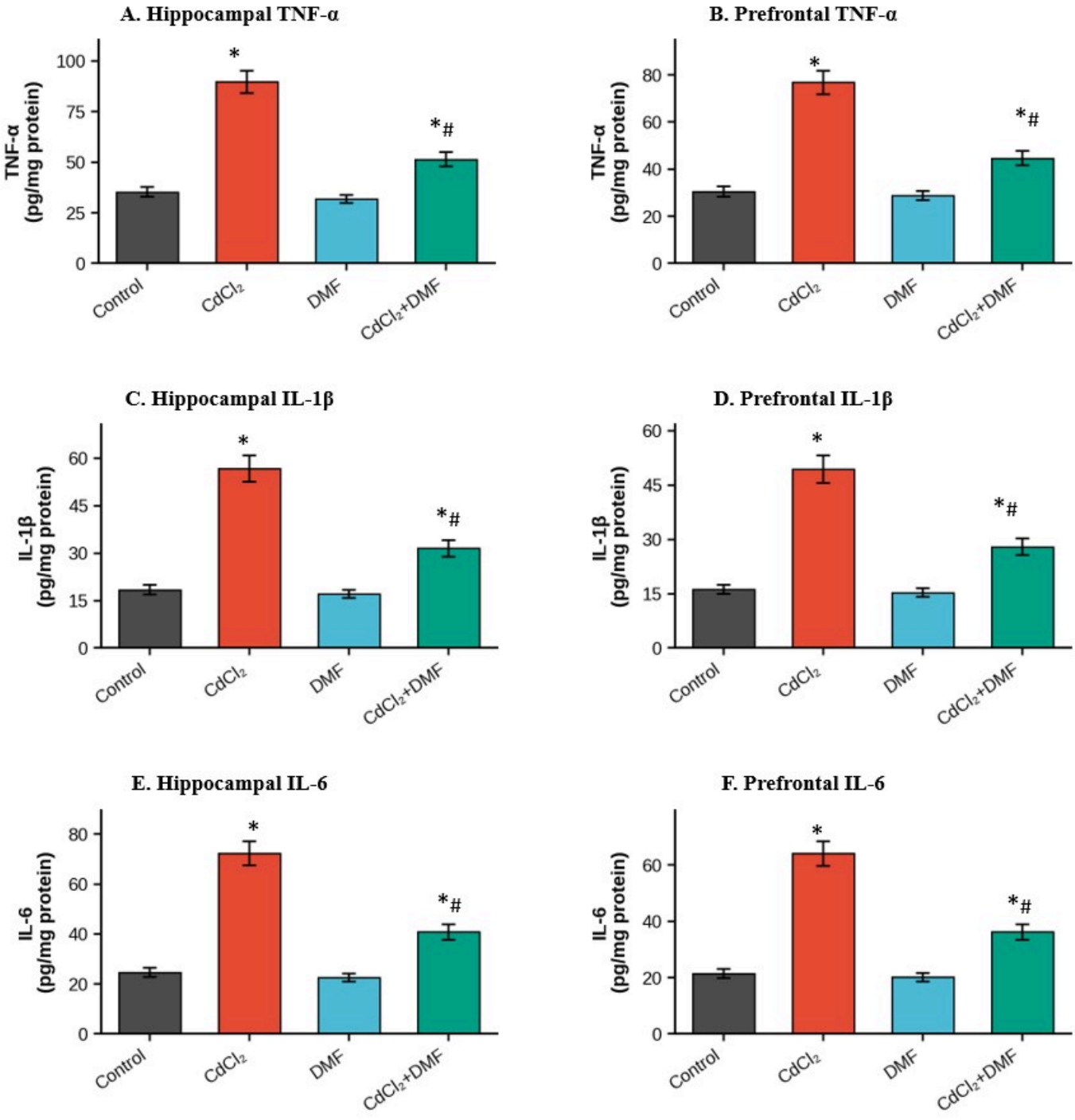


Figure 2

Effects of $CdCl_2$ and dimethyl fumarate on pro-inflammatory cytokines in the hippocampus and prefrontal cortex. TNF-α, IL-1β and IL-6 concentrations were increased following $CdCl_2$ exposure and significantly attenuated by DMF co-treatment in both brain regions. Data are presented as mean ± SD (n = 8 rats/group). Group differences were analysed using one-way ANOVA followed by Tukey's multiple-comparison test. *p < 0.05 versus Control; #p < 0.05 versus $CdCl_2$. $CdCl_2$, cadmium chloride; DMF, dimethyl fumarate; TNF-α, tumour necrosis factor-α; IL-1β, interleukin-1β; IL-6, interleukin-6

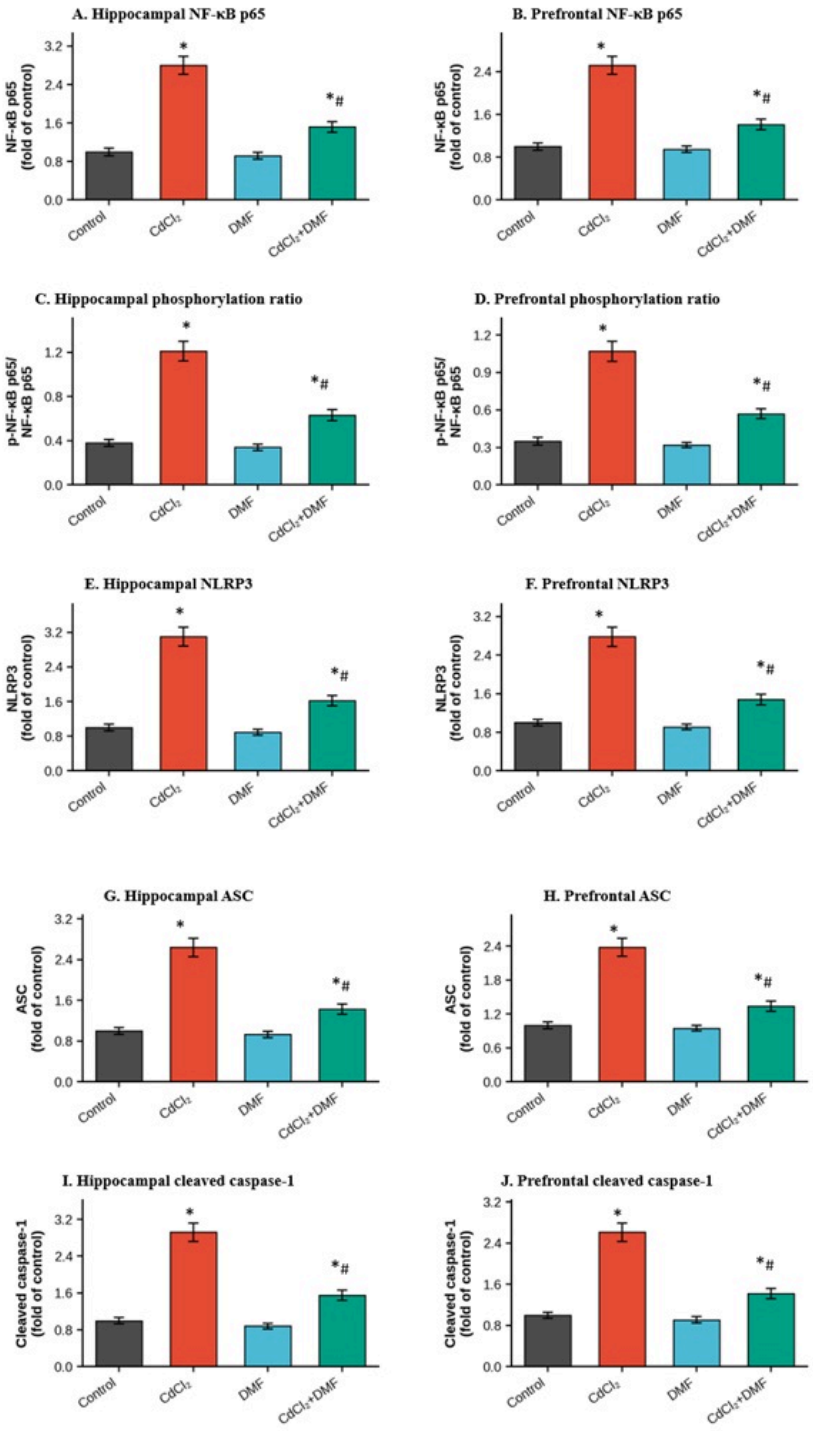


Figure 3

Effects of $CdCl_2$ and dimethyl fumarate on NF-κB/NLRP3 inflammasome-associated signalling in the hippocampus and prefrontal cortex. $CdCl_2$ increased NF-κB p65 expression, the p-NF-κB p65/NF-κB p65 ratio, NLRP3, ASC and cleaved caspase-1 in both brain regions, whereas DMF co-treatment significantly attenuated these changes. Data are presented as mean ± SD (n = 8 rats/group). Group differences were analysed using one-way ANOVA followed by Tukey's multiple-comparison test. *p < 0.05 versus Control;

#p < 0.05 versus $CdCl_2$. $CdCl_2$, cadmium chloride; DMF, dimethyl fumarate; NF-κB, nuclear factor kappa B; NLRP3, NLR family pyrin domain-containing protein 3; ASC, apoptosis-associated speck-like protein containing a CARD.

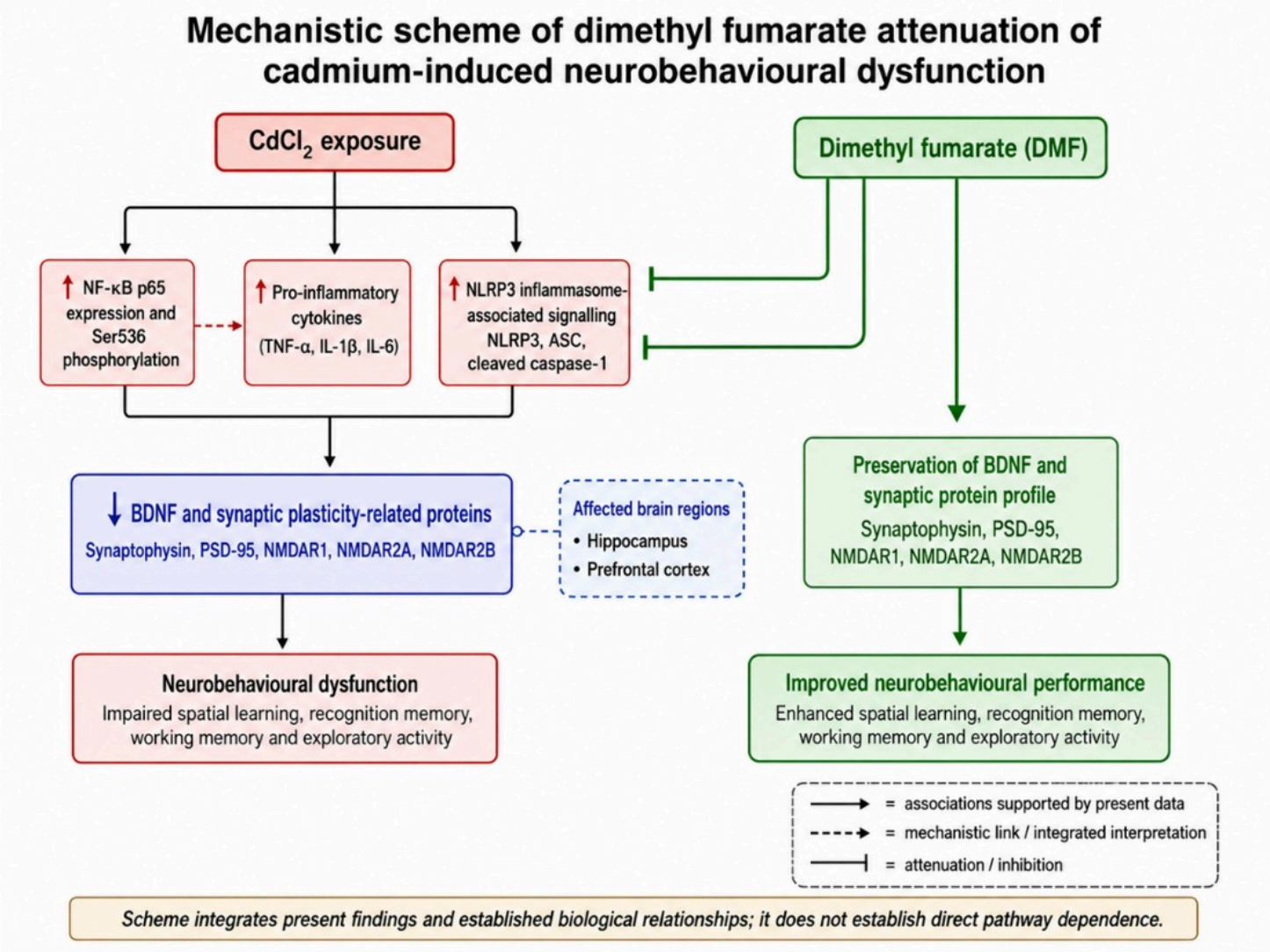


Figure 4

Mechanistic scheme of dimethyl fumarate attenuation of cadmium-induced neurobehavioural dysfunction.